RAPID COMMUNICATIONS

PHYSICAL REVIEW E VOLUME 53, NUMBER 4 APRIL 1996

Detection of THz pulses by phase retardation in lithium tantalate

P. Uhd Jepsen,* C. Winnewisser, M. Schall, V. Schyja, S. R. Keiding,* and H. Helm
Fakultät für Physik, Albert-Ludwigs-Universität, Hermann-Herder-Strasse 3, D-79104 Freiburg, Germany
(Received 22 September 1995)

Freely propagating THz pulses are recorded in a thin lithium tantalate crystal by monitoring the phase retardation of a femtosecond probe pulse. This technique permits the determination of the temporal shape of the THz pulse in the picosecond time domain and offers the exciting prospect of up-converting the spatial THz beam profile into the optical wavelength range in real time, with potential application in diagnostics.

PACS number(s): 42.25.−p, 42.65.Re

In the last decade, the physics of short-pulse THz radiation has become an active research field, with interest both in fundamental aspects of generation and detection of THz radiation and in spectroscopic applications [1]. Existing applications include time-domain spectroscopy of liquids, gases, and semiconductor materials as well as transmission studies (T-ray imaging) [2]. In these experiments a broadband, low-power coherent THz emitter, driven by femtosecond (fs) laser pulses is used at a high repetition rate. Radiation is then emitted in short bursts containing frequencies from a few GHz to several THz. These THz pulses are detected by an optically gated photoconductive switch; frequently a radiation damaged silicon-on-sapphire (SOS) stripline detector is used [1].

With the advent of high-power fs lasers it has become possible to generate THz pulses with high peak power. The high peak power gives the opportunity to use the THz pulse as a pump pulse, as opposed to a weak, noninteracting probe [3–5]. High-power THz pulses are generated by illuminating a large-aperture semiconductor emitter with a large external bias field applied across the gap. The photocarriers produced by the laser pulse are accelerated by the bias field, resulting in a large transient surface current. An electromagnetic pulse proportional to the time derivative of this current is radiated [4,5]. Peak THz-field strengths up to 150 kV/cm (vacuum) have been demonstrated, corresponding to pulse energies of 0.8 μJ [6].

Due to the low repetition rate of amplified high-power laser systems, typically from 10 Hz to a few kHz, the noise level limits the detection sensitivity for THz radiation compared to the low-power, high repetition rate systems. A sensitive method to detect high-power THz pulses employs a Michelson interferometer, measuring the output energy with a cooled bolometer while scanning one arm of the interferometer. With this method, it is possible to detect the temporal shape of even very short pulses [7], limited by the thermal noise of the bolometer. It is also possible to detect the pulses in a gated photoconductive switch applied in low-power THz experiments [4,5]. This detector can be operated at room temperature, but operation at low repetition rate requires a larger detection area, which in turn cuts off the detector response at high frequencies.

Here we describe and demonstrate a method for detecting freely propagating THz pulses, based on the electro-optic effect in lithium tantalate ($LiTaO_3$). A change in the index of refraction occurs in the crystal, when an electric field is applied to the crystal. With the proper orientation, it is possible to obtain different index changes along the different axes in the crystal, an effect well known in its application in a Pockel's cell [8].

We show that it is possible to introduce a phase retardation between two propagation axes in a $LiTaO_3$ crystal by exposing the crystal to a freely propagating THz pulse. The induced phase retardation (PR) is probed by a weak laser pulse. The phase retardation signal obtained by varying the time delay between the THz pulse and the probe pulse corresponds closely to the time integral of the THz pulse shape. In pioneering work in 1972, Auston and Glass used the electro-optic effect to visualize the temporal shape of a picosecond electrical pulse in a $LiTaO_3$ rod [9]. In 1982, Valdmanis *et al.* carried out similar studies in lithium niobate [10]. Later, Auston and Nuss studied the optical properties of $LiTaO_3$ in the THz range by generation of Cherenkov radiation inside the crystal [11]. Common to these experiments is that they characterize electrical pulses generated inside the electro-optic medium. In our case an external THz pulse is injected into the crystal.

We illustrate the basic physics of our phase retardation experiment in Fig. 1. The uniaxial $LiTaO_3$ crystal is oriented with the ordinary and extraordinary axes, with indices n_o and n_e, respectively, in the plane of the crystal surface. The THz beam and the probe beam propagate collinearly through the crystal along the z direction (index n_o). The polarization of the THz beam is kept parallel to the extraordinary axis. The probe beam is linearly polarized at 45° with respect to the ordinary and extraordinary axes. Linearly polarized light becomes elliptically polarized due to the natural birefringence of the crystal:

$$\Delta\phi_{nat}=\frac{\omega}{c}(n_e-n_o)L, \tag{1}$$

where ω is the probe beam frequency and L is the length of the crystal. In the presence of an electric field (the THz field), an additional phase change, $\Delta\phi_{THz}$, will be introduced between the two electrical field components of the probe pulse,

*Permanent address: Kemisk Institut, Århus Universitet, Langelandsgade 140, 8000 Århus C, Denmark.

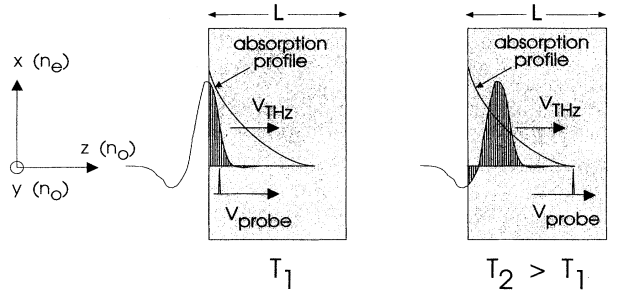

FIG. 1. Principle of the phase retardation detection technique. Due to the difference in the refractive indices (≈factor 3) the probe pulse sweeps across the electrical field profile of the THz pulse inside the crystal. The total phase change experienced by the probe beam is proportional to the shaded area of the THz pulse convolved with the THz absorption profile. The length L is the crystal thickness. The probe pulse and the THz pulse propagate collinear into the crystal, in the z direction. The refractive indices in the directions (x,y,z) are (n_e,n_o,n_o), respectively.

$$\Delta\phi_{THz}(T)=\frac{1}{2}\frac{\omega}{c}(n_o^3 r_{13}-n_e^3 r_{33})\int_0^L E_{THz}\left(\frac{z}{c}\Delta n+T\right)\times e^{-\alpha z}dz, \tag{2}$$

where r_{13} and r_{33} are components of the electro-optic tensor for $LiTaO_3$ [8]. The integral over the electric field of the THz beam accounts for a situation where the THz beam is attenuated inside the crystal (coefficient α) and where the probe pulse propagates much faster through the crystal than the THz pulse ($\Delta n=n_{probe}-n_{THz}\approx -4.35$ [11]). Therefore the probe pulse effectively sweeps over the portion of the THz pulse that lies inside the crystal. Implicit in Eq. (2) is the assumption that the duration of the probe pulse is much shorter than that of the THz pulse, a condition fullfilled in our experiment (140 fs vs 2 ps). The relative time delay between the THz pulse and the probe pulse is represented by the parameter T. Converting the integration over length into one over time, Eq. (2) can be rewriten as

$$\Delta\phi_{THz}(T)=\frac{1}{2}\frac{\omega}{c}(n_o^3 r_{13}-n_e^3 r_{33})\frac{c}{\Delta n}\int_T^{T+(\Delta nL/c)} E_{THz}(t)\times\exp\left(-\frac{\alpha c}{\Delta n}(t-T)\right)dt. \tag{3}$$

If it is assumed that the attenuation coefficient, α, is frequency independent, one can extract the temporal shape of the THz pulse directly from the measured phase change $\Delta\phi_{THz}(T)$ by differentiating Eq. (3):

$$E_{THz}(T)\propto\frac{d}{dT}\Delta\phi_{THz}(T)-\frac{\alpha c}{\Delta n}\Delta\phi_{THz}(T). \tag{4}$$

In Eq. (4) we use the fact that $\Delta nL/c$ (15 ps in our setup) is long compared to the time duration of the THz pulse. $LiTaO_3$ is known to strongly absorb at high frequencies [11] due to a lattice resonance at 6.23 THz. However, the data in [11] show that attenuation is small up to frequencies of ~1 THz, leaving the second term on the right hand side of Eq. (4) as a small correction at low frequencies.

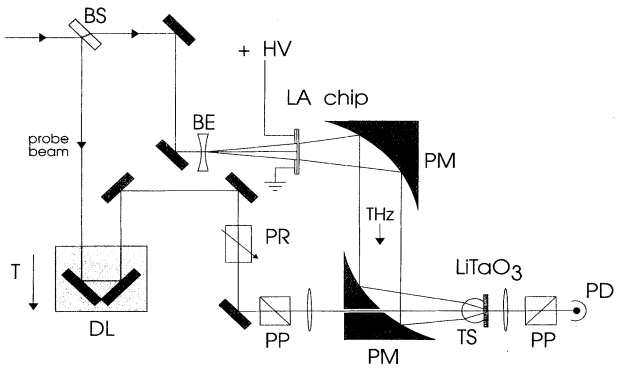

FIG. 2. Schematic illustration of the setup. Legend: BS–10% beam splitter, BE–beam expander, LA chip–large aperture emitter chip (1 cm), PM–off-axis paraboloidal mirrors, DL–delay line, PR–polarization rotator, PP–polarizing prisms, TS–truncated, spherical sapphire lens.

To detect the small phase retardation from Eq. (3), the electro-optic crystal is placed between a pair of crossed polarizers. The laser beam, which generates the THz pulses, is chopped and the diode signal is monitored by lock-in techniques. The output signal behind the second polarizer is calculated to be proportional to $\Delta\phi_{THz}$ [8]:

$$V_{diode}\propto\Delta\phi_{THz}\sin\Delta\phi_{nat}+O(\Delta\phi_{THz}^2\cdots), \tag{5}$$

where $O(\Delta\phi_{THz}^2\cdots)$ are higher orders terms of $\Delta\phi_{THz}$.

Figure 2 presents a schematic drawing of the experimental setup. The laser source is a Ti:sapphire oscillator, amplified in a chirped pulse regenerative amplifier at a repetition rate of 1 kHz (Clark MXR). We use only a small fraction of the available pulse energy, since the THz signal emitted from the large-aperture emitter saturates at incident energies of a few μJ. The emitter consists of a wafer of high resistivity GaAs ($\rho>10^7$ Ω cm), with electrodes painted on the surface with conducting silver paint, leaving an emitter area of 1 cm^2. The THz radiation is collimated by a pair of off-axis paraboloidal mirrors, which guide the THz radiation to the crystal. The thickness of the crystal is 1 mm. A truncated, spherical sapphire lens of 5 mm radius is attached directly to the crystal to focus the THz radiation [12]. The full width at half maximum of the THz beam field distribution at the crystal surface is estimated to lie between 50 and 100 μm [13]. A lens is used to optimize the size of the probe beam with respect to the THz beam inside the crystal.

Phase retardation signals in $LiTaO_3$ were measured over a range of peak electric field strengths. A typical phase retardation signal obtained with a peak THz field strength of 2.4 kV/cm is shown in Fig. 3(a) as a function of the time delay between the THz pulse and the probe pulse. The maximum signal amplitude of 10 μV corresponds to a phase retardation of $\Delta\phi_{THz}=0.3°$. Using the electro-optic coefficients $r_{13}=8pm/V$ and $r_{33}=30pm/V$, the refractive indices $n_o=2.154$ and $n_e=2.158$ [14], and $\alpha=0$ Eq. (3) predicts a

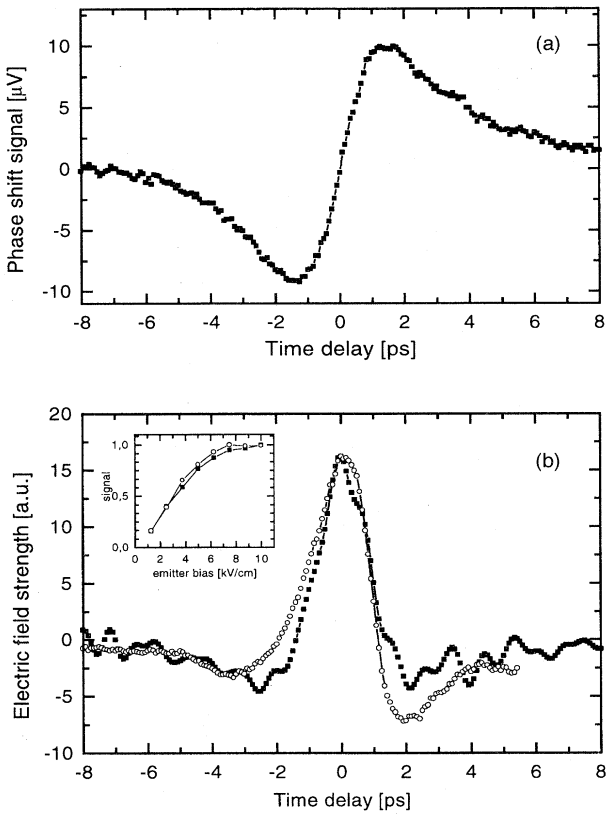

FIG. 3. (a) The phase retardation (PR) signal, as a function of the time delay T. The maximum signal of 10 μV corresponds to a phase retardation of 0.3°. (b) The differentiated PR signal (filled squares) is shown in comparison to the silicon-on-sapphire (SOS) detector signal (open circles). The differentiated PR signal has been smoothed, and the SOS signal has been normalized with respect to the differentiated PR signal. The inset gives the THz peak emitted field strength saturation as a function of the emitter bias field, as measured by the two independent methods.

maximum PR of 0.5°, in overall agreement with our direct measurement.

In Fig. 3(b), the derivative of the PR signal is shown, together with the pulse shape measured directly with an SOS detector inserted in place of the $LiTaO_3$ crystal in Fig. 2. For negligiable absorption the differentiated retardation signal[first term on the right hand side of Eq. (4)] should reveal the temporal distribution of the the THz field strength. There is a good correspondence between the SOS signal and the differentiated PR signal. The differentiated signal has been smoothed, and the SOS signal has been scaled to the differentiated PR signal. The oscillations seen in the direct and differentiated PR signal before and after the main peak are reproducible, but their origin is not understood at present.

The inset in Fig. 3(b) compares the normalized peak field strengths obtained from the SOS detection and the differentiated phase retardation signal, as functions of the applied field strength to the emitter, in the range from 1.25 kV/cm to 10 kV/cm. Both curves show similar response to the emitter bias field, indicative of the linear response of the PR detection technique.

We have described an alternative setup for the detection of freely propagating THz pulses, and compared its performance to that of the conventional SOS detector. At present, the signal to noise (S/N) ratio is lower than that of the photoconductive detection technique, but other geometries of the polarizer section for the PR detection will improve the S/N ratio. While the absorption of the high frequency components of the THz pulse limits the analysis (though not the detection) of the full frequency spectrum of the THz pulse, in $LiTaO_3$, other materials may emerge with broader frequency response.

The PR detection demonstrated here may serve as the basic principle to characterize the spatial profile of THz beams. In such an experiment, one will use the fact that the spatial beam profile of the focused THz beam inside the crystal gives rise to a spatially dependent PR signal. Thus, the transmitted optical probe beam inherently contains the spatial information of the THz beam. Experiments to extract this information are currently under way.

This research was supported by the Deutsche Forschungsgemeinschaft through SFB 276, TP C14. We thank Dr. G. Alber for helpful discussions.

[1] D. Grischkowsky, S. Keiding, M. van Exter, and Ch. Fattinger, J. Opt. Soc. Am. B **7**, 2006 (1990).

[2] B. B. Hu and M. C. Nuss, Opt. Lett. **20**, 1716 (1995).

[3] J. T. Darrow, X.-C. Zhang, D. H. Auston, and J. D. Morse, IEEE J. Quantum Electron. **28**, 1607 (1992).

[4] R. R. Jones, D. You, and P. H. Bucksbaum, Phys. Rev. Lett. **70**, 1236 (1993).

[5] P. K. Benicewicz, J. P. Roberts, and A. J. Taylor, J. Opt. Soc. Am. B **11**, 2533 (1994).

[6] D. You, R. R. Jones, P. H. Bucksbaum, and D. R. Dykaar, Opt. Lett. **18**, 290 (1993).

[7] B. I. Greene, J. F. Federici, D. R. Dykaar, R. R. Jones, and P. H. Bucksbaum, Appl. Phys. Lett. **59**, 893 (1991).

[8] B. E. A. Saleh and M. C. Teich, in *Fundamentals of Photonics*, edited by J. W. Goodman (John Wiley & Sons, Inc., New York, 1991).

[9] D. H. Auston and A. M. Glass, Appl. Phys. Lett. **20**, 398 (1972).

[10] J. A. Valdmanis, G. Mourou, and C. W. Gabel, Appl. Phys. Lett. **41**, 211 (1982).

[11] D. H. Auston and M. C. Nuss, IEEE J. Quantum Electron. **24**, 184 (1988).

[12] Ch. Fattinger and D. Grischkowsky, Appl. Phys. Lett. **54**, 490 (1989).

[13] P. Uhd Jepsen, R. H. Jacobsen, and S. R. Keiding (unpublished).

[14] Landolt-Börnstein, in *Numerical Data and Functional Relationships in Science and Technology*, **III/3**, edited by K.-H. Hellwege (Springer-Verlag, Berlin-Heidelberg, 1969).

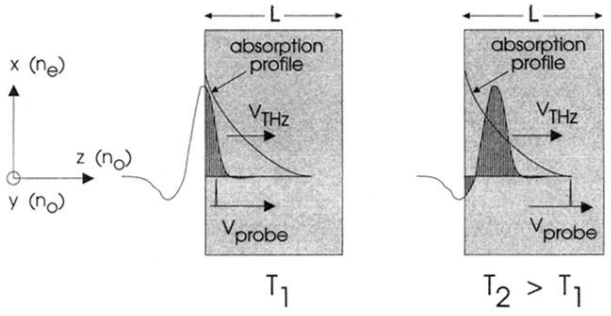

FIG. 1. Principle of the phase retardation detection technique. Due to the difference in the refractive indices ($\approx$factor 3) the probe pulse sweeps across the electrical field profile of the THz pulse inside the crystal. The total phase change experienced by the probe beam is proportional to the shaded area of the THz pulse convolved with the THz absorption profile. The length L is the crystal thickness. The probe pulse and the THz pulse propagate collinear into the crystal, in the z direction. The refractive indices in the directions (x,y,z) are (n_e,n_o,n_o), respectively.

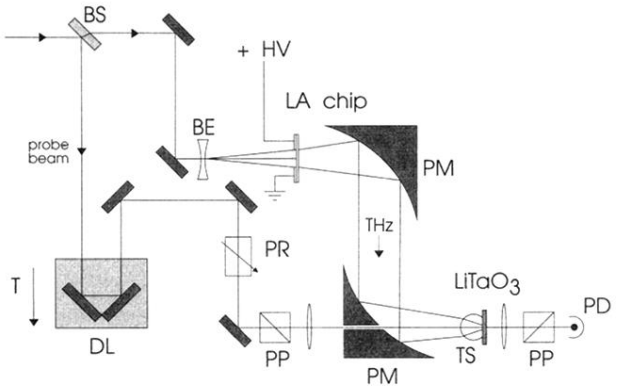

FIG. 2. Schematic illustration of the setup. Legend: BS–10% beam splitter, BE–beam expander, LA chip–large aperture emitter chip (1 cm), PM–off-axis paraboloidal mirrors, DL–delay line, PR–polarization rotator, PP–polarizing prisms, TS–truncated, spherical sapphire lens.